Ultrasound in Med. & Biol., Vol. 32, No. 6, pp. 915–924, 2006

0301-5629/06/$–see front matter

ELSEVIER

doi:10.1016/j.ultrasmedbio.2006.02.1416

● *Original Contribution*

MECHANISM OF INTRACELLULAR DELIVERY BY ACOUSTIC CAVITATION

ROBYN K. SCHLICHER,*† HARISH RADHAKRISHNA,‡ TIMOTHY P. TOLENTINO,*
ROBERT P. APKARIAN,§ VLADIMIR ZARNITSYN,† and MARK R. PRAUSNITZ,*†

*The Wallace H. Coulter Department of Biomedical Engineering at Georgia Tech and Emory University, Georgia Institute of Technology; †School of Chemical & Biomolecular Engineering, Georgia Institute of Technology; ‡School of Biology, Georgia Institute of Technology; and §Integrated Microscopy & Microanalytical Facility, Emory University, Atlanta, Georgia, USA

(*Received* 22 *August* 2005; *revised* 24 *January* 2006; *in final form* 31 *January* 2006)

Abstract—Using conditions different from conventional medical imaging or laboratory cell lysis, ultrasound has recently been shown to reversibly increase plasma membrane permeability to drugs, proteins and DNA in living cells and animals independently of cell or drug type, suggesting a ubiquitous mechanism of action. To determine the mechanism of these effects, we examined cells exposed to ultrasound by flow cytometry coupled with electron and fluorescence microscopies. The results show that cavitation generated by ultrasound facilitates cellular incorporation of macromolecules up to 28 nm in radius through repairable micron-scale disruptions in the plasma membrane with lifetimes >1 min, which is a period similar to the kinetics of membrane repair after mechanical wounding. Further data suggest that cells actively reseal these holes using a native healing response involving endogenous vesicle-based membrane resealing. In this way, noninvasively focused ultrasound could deliver drugs and genes to targeted tissues, thereby minimizing side effects, lowering drug dosages, and improving efficacy. (E-mail: prausnitz@gatech.edu) **© 2006 World Federation for Ultrasound in Medicine & Biology.**

Key Words: **Ultrasound, Intracellular drug delivery, Cell membrane wound repair, Electroporation, Endocytosis.**

INTRODUCTION

Traditional drug delivery methods, such as injections and oral medications, are often unsuitable for proteins, DNA, and other biotherapeutic compounds (Langer 1998). Drug delivery methods need improvement to increase drug and gene efficacy by enhancing intracellular delivery and to increase drug safety by targeting specific cells or organs to reduce side effects. Enhanced and targeted delivery methods are both limited by insufficient or uncontrolled transport across cell membranes. To address these delivery problems, ultrasound has been used to increase plasma membrane permeability and thereby load living cells with drugs, proteins and genes (Fechheimer et al. 1987; Dalecki 2004; Tachibana 2004). *In vivo* experiments have demonstrated targeted delivery of chemotherapeutic agents to tumors (Gao et al. 1996; Tomizawa et al. 2001; Yuh et al. 2005), enhanced expression of DNA in tissues (Huber et al. 2003; McCreery et al. 2004; Bekeredjian et al. 2005) and increased transdermal delivery of proteins (Mitragotri and Kost 2004).

Despite proof of principle that ultrasound offers compelling opportunities to enhance therapy, progress in the field has been limited by an insufficient understanding of ultrasound's mechanism of action. It has been shown that ultrasound's bioeffects are caused by bubble collapse during acoustic cavitation, which releases energy that temporarily increases the internalization of exogenous molecules by living cells and sometimes renders other cells nonviable (Dalecki 2004; Tachibana 2004). These bioeffects are influenced by acoustic as well as other parameters, where increased acoustic energy and presence of cavitation nucleation sites generally increase bioeffects (Guzman et al. 2003; Larina et al. 2005). However, it is not fully known how molecules enter cells and what ultrasonic cavitation does to cells to facilitate intracellular uptake.

§ Author Robert P. Apkarian is deceased.

Address correspondence to: Mark R. Prausnitz, School of Chemical and Biomolecular Engineering, Georgia Institute of Technology, 311 Ferst Drive, Atlanta, GA 30332-0100. E-mail: prausnitz@gatech.edu

The literature does contain information about cavitation's damaging biologic effects to lyse cells in the biotechnology laboratory (Rapley and Walker 1998) and shatter kidney stones in clinical lithotripsy (Hill et al. 2004). However, this study addresses the milder bioeffects of acoustic cavitation, where the cell membrane can be reversibly disrupted to facilitate intracellular uptake of macromolecules into living cells (Ohl and Wolfrum 2003; van Wamel et al. 2004; Prentice et al. 2005). To determine this mechanism, experimental design and data analysis were guided by three candidate mechanisms for ultrasound-induced uptake. The first candidate mechanism is active transport via endocytosis, where endogenous cellular machinery, *e.g.*, surface receptor sites such as caveoli, could be upregulated and thus cause internalization of molecules in plasma membrane invaginations that form internalized vesicles (Yeagle 1993).

The second candidate mechanism involves passive transport through transient, nanometer pores in the plasma membrane similar to those caused by electroporation (Chang et al. 1992). In this scenario, water is forced into the cell membrane, which causes a molecular rearrangement of the lipid bilayers to accommodate a hydrophilic pore through the otherwise hydrophobic lipid membrane (Weaver and Chizmadzhev 1996). These pores are believed to be 1 to 10 nm in size and spontaneously reseal after milliseconds to minutes. In contrast to active cellular processes, this mechanism is a physical process based on hydrophilic-hydrophobic interactions that do not require active involvement of the cell to form or reseal the resulting holes.

The final candidate mechanism involves uptake through actively repairable "wounds" in the plasma membrane, similar to those known to be formed by other physical stresses applied to cells (McNeil and Steinhardt 2003). It has been shown that suspended cells exposed to shear forces in high-velocity flows or adherent cells rapidly detached from their substrate can have their plasma membrane removed in patches measuring up to microns in size. Cells reseal these wounds by an active process involving trafficking of intracellular vesicles to the site of injury, where vesicle fusion reseals the membrane on a timescale of minutes.

MATERIALS AND METHODS

Ultrasound apparatus

Samples were exposed to ultrasound in a chamber made from a cylindrical piezoelectric transducer (Channel Industries, Santa Barbara, CA, USA) sealed between two PVC pipes (5.1 cm inner diameter), as described previously (Cochran and Prausnitz 2001). The chamber was filled with deionized water that had been degassed for 2 h using a bell jar (Nalgene, Rochester, NY, USA) and vacuum pump (KNF Neuberger, Trenton, NJ, USA) to remove bubble nucleation sites and thereby reduce cavitation in the water bath that could alter the pressure field in the sample chamber.

Ultrasound was generated at 24 kHz by a function generator (DS354 SRI, Stanford Research Systems, Sunnyvale, CA, USA) and amplifier (Macro-Tech 2410, Crown Audio, Elkhart, IN, USA) that controlled the transducer via a matching transformer (MT-56R, Krohn-Hite, Avon, MA, USA). Parameters including the frequency, duty cycle, incident pressure, pulse length and exposure time were set using this system. The incident pressure was determined using a calibrated hydrophone (Model 8103, Brüel and Kjær, Norcross, GA, USA); radial variability in pressure across the width of the cell sample chamber (9 mm wide) was less than 10% and axial variability up and down the cell sample chamber height (21 mm tall) was less than 20% (Cochran and Prausnitz 2001).

Cell culture

DU 145 prostate-cancer cells (American Type Culture Collection, Manassas, VA, USA) were grown to 80% confluence on T-150 flasks (BD Falcon, Franklin Lakes, NJ, USA) in growth media (RPMI 1640, Cellgro, Herndon, VA, USA) supplemented with 10% fetal bovine serum (Cellgro or Atlanta Biologicals, Atlanta, GA, USA) at 37°C, 5% CO_2, and 90% relative humidity before harvest during exponential growth by trypsinization using standard protocols.

Cell pretreatments

To measure intracellular uptake, solutions of fluorescent marker compounds were added to cell suspensions before sonication at final concentrations of 10 μM calcein (unless otherwise noted) (Molecular Probes, Eugene, OR, USA), 10 μM FITC-labeled bovine serum albumin (Molecular Probes), 10 μM FITC-labeled 150-kDa dextran, 1 μM FITC-labeled 500-kDa dextran or 0.1 μM FITC-labeled 2,000-kDa dextran (Sigma, St. Louis, MO, USA). Fluorescence from marker compounds retained within cells was measured by flow cytometry, as described below.

To measure release of a marker compound from the cytosol, cells were incubated at room temperature for 15 min in 100 nM calcein AM (Molecular Probes), washed with RPMI 1640 to remove excess calcein AM and sonicated immediately after this treatment in fresh RPMI 1640 media.

To identify nonviable cells after sonication, and eliminate them from analysis, propidium iodide (Molecular Probes), which stains the nuclei of nonviable, membrane-compromised cells with red fluorescence, was

added to samples at a final concentration of 0.15 μM before assaying with flow cytometry.

To deplete cells of ATP, cells were incubated in RPMI 1640 with 0.05% (w/v) sodium azide and 50 μM 2-deoxyglucosidase (Sigma) for 30 min at 37°C (Gonzalez-Dunia et al. 1998). Cells were sonicated in the treatment media in the presence of 10 μM calcein and then washed with phosphate-buffered saline (PBS).

To deplete cells of intracellular Ca^{2+}, cells were incubated in RPMI 1640 with 50 μM BAPTA AM in DMSO (Sigma) for 20 min at 37°C (Chen et al. 2002). Afterwards, cells were washed and sonicated in PBS (without calcium and magnesium) in the presence of 10 μM calcein.

To deplete cells of K^+, cells were washed with K^+-free buffer (140 mM NaCl, 1 mM $CaCl_2$, 1 mM $MgCl_2$, 1 mg/mL D-glucose in DI H_2O, pH 7.4) followed by hypotonic shock for 5 min in K^+-free buffer diluted 1:1 with DI water (Larkin et al. 1983). Cells were sonicated in K^+-free buffer in the presence of 10 μM calcein.

To serve as negative controls, cells were prepared identically and simultaneously with each of these pretreatment depletion protocols, but exposed only to "sham" ultrasound (*i.e.*, acoustic pressure equal to zero). To serve as positive controls, cells were prepared according to the "standard" protocol without depletion pretreatment and exposed to ultrasound under conditions identical to experimental samples.

To examine the role of endocytosis, plasma membranes were selectively labeled by preincubation of cells for 30 min in RPMI 1640 (with serum) containing 10 μM FM 1-43 (Molecular Probes) supplied from a stock solution of 1 mM FM 1-43 in dimethylsulfoxide (DMSO). This preincubation was carried out at 2°C to suppress endocytotic internalization of labeled lipids during the labeling procedure. FM 1-43 is believed to reversibly insert itself into the outer leaflet of the plasma membrane and, when internalized in invaginated membrane vesicles during subsequent sonication experiments, causes a large increase in overall cell fluorescence, which serves as an indicator of endocytosis (Cochilla et al. 1999). After cells were washed with RPMI 1640 (with serum) to remove excess FM 1-43, they were sonicated in RPMI 1640 (with serum) to determine whether endocytosis is upregulated by exposure to ultrasound and assayed by flow cytometry. Because of the spectral overlap of FM 1-43 with propidium iodide, propidium iodide was not added before flow cytometry as a viability marker.

Loss of intracellular vesicles by exocytosis or other mechanisms was studied by long-term incubation of adherent cells in RPMI 1640 (with serum) containing 10 μM FM 1-43 for 12 to 16 h at 37°C. This long incubation allowed endocytotic internalization of large amounts of dye-labeled vesicles. Subsequent loss of these vesicles by rejoining the plasma membrane or otherwise leaving the cell causes overall cellular fluorescence to become less bright (Togo et al. 1999). After labeling in this way, cells were harvested from the growth surface by trypsinization, followed by sonication in RPMI 1640 media (with serum) and assayed using flow cytometry and confocal microscopy.

Ultrasound exposure

Well-mixed cell suspensions at a concentration of 10^6 cells/mL in RPMI 1640 (with serum, unless noted) or sonication buffers (in those special cases described above) were gently introduced into 1.2-mL sample chambers (No. 241 SEDI-PET transfer pipets with stems cut to 2 cm in length, SAMCO, San Fernando, CA, USA) with a 22-gauge needle and 3-mL syringe (Becton-Dickinson, Franklin Lakes, NJ, USA), ensuring that no bubbles were introduced into the sample chamber. After completely filling the chamber, a stainless steel rod (1.6 mm diameter) was carefully inserted into the stem to avoid introducing air into the sample. Sample chambers were then positioned in the exposure chamber water bath by clamping the end of the steel rod at a location that positioned the sample chamber in the axial and radial center of the transducer. Most samples (unless noted) were sonicated using 20 acoustic pulses each at 24 kHz, 7 atm, and 0.1 s pulse length at 10% duty cycle. As negative controls, "sham" samples were prepared identically, but no ultrasound was applied.

After ultrasound exposure, cells were allowed to "recover" at room temperature for 5 to 10 min and then washed 2 times with Dulbecco's PBS (Cellgro) by centrifugation (735*g*, 4 min, Eppendorf 5415 C, Brinkmann Instruments, Westbury, NY, USA) at room temperature and resuspended in PBS. Samples were stored on ice for as long as 1 h until they were assayed by flow cytometry.

Erythrocyte ghosts

Erythrocyte ghosts were prepared from red blood cells isolated from bovine blood preserved with Alsevers (Rockland Immunoproducts, Gilbertsville, PA, USA) and then exposed to hypotonic shock in 5 mM phosphate buffer for 2 h (Dodge et al. 1963). Ghosts at a concentration of 10^7 erythrocyte ghosts/mL in PBS were exposed to ultrasound as described above at 2 to 8 atm and to electroporation (ECM 600, BTX Instruments, Holliston, MA, USA) using four 1-ms, 2-kV/cm pulses in the presence of 10 μM calcein (Prausnitz et al. 1993).

Flow cytometry assay

Samples were run on a BD-LSR flow cytometer using FACS DiVa software (BD Biosciences, Franklin

Lakes, NJ, USA). The fluorescence of green marker compounds (including calcein, calcein AM, FITC-labeled compounds and FM 1-43 labeled membranes) was measured with a 488-nm argon laser excitation and a 530/30 bandpass filter for emission. Red-fluorescent propidium iodide was also excited at 488 nm and measured using a 675/20-nm bandpass filter for emission. Intracellular uptake levels were quantified by converting to an average number of molecules per cell using calibration beads (Quantum 25, Flow Cytometry Standards Corporation, San Juan, Puerto Rico or Bangs Labs, Fishers, IN, USA) (Prausnitz et al. 1993).

Microscopy assays

Cell samples viewed by electron microscopy were fixed with 2.5% EM-grade glutaraldehyde (Sigma) either 2 s or 30 s after sonication and prepared using standard techniques (Castejon et al. 2001) for viewing by conventional scanning electron microscopy (SEM) (DS-130 field emission SEM, Topcon, Tokyo, Japan) or transmission electron microscopy (TEM) (JEOL 1210 LaB6, Peabody, MA, USA).

To prepare cells for confocal laser-scanning imaging, samples were labeled with one or both of the following dyes: cell membranes were labeled by incubating in 2 mM TRITC- or FITC-labeled wheat germ lectin (Sigma) for 20 min at 2°C (Sharon and Lis 1989) and intracellular vesicles were labeled with FM 1-43 as described above. After washing off residual dye, cells were sonicated in fresh RPMI 1640 with 100 μM calcein or 0.15 μM propidium iodide. Before analysis by confocal microscopy (Zeiss LSM 510, Thornwood, NY, USA), some samples were fixed in glutaraldehyde (Sigma) either 2 s or 30 s after sonication, whereas other samples were imaged in real time immediately after sonication.

RESULTS

Ultrasound facilitates uptake and retention of molecules present during sonication and introduced after sonication ends

We studied uptake of fluorescent molecules into DU 145 prostate cancer cells during and after ultrasound exposure at pressures greater than the cavitation threshold. Molecules span a range of sizes (0.6 to 2,000 kDa) and a variety of structures, including a protein and several dextrans. Confocal microscopy (Fig. 1) showed that all of the molecules were transported into the cytosol of living cells when present in the media during sonication. However, only calcein, a molecule smaller than the nuclear pore diameter (Keminer and Peters 1999), appears in the nucleus at high concentration, suggesting that ultrasound-mediated uptake effects are limited to the plasma membrane.

The effects on these "uptake" cells appear to be reversible, as indicated by two assays of cellular function. As a short-term viability assay, propidium iodide was excluded from uptake cells when added ~30 min after sonication (data not shown). Propidium iodide is normally excluded from viable cells, but enters and stains nonviable cells (Arndt-Jovin and Jovin 1989). As a longer-term assay, uptake cells exposed under similar conditions were also seen to retain their ability to undergo mitosis when returned to physiologic conditions after sonication (Zarnitsyn and Prausnitz 2004).

Flow cytometry analysis of sonicated cells showed that 10 to 40% had increased fluorescence indicative of molecular uptake (Fig. 1b), consistent with previous observations (Guzman et al. 2001). Intracellular concentration of low-molecular weight calcein in these "uptake populations" approached equilibrium with the extracellular concentration and the macromolecules reached 4 to 39% of the extracellular concentration (Fig. 1c). Such high intracellular concentrations indicate that transmembrane transport was extensive. Lesser uptake of larger molecules can be explained by lower effective diffusivity due to larger molecular size and greater hindrance by intracellular structures.

A study of postexposure molecular uptake was performed by adding sonicated samples of DU 145 cells to fluorescent solutions at known increments of time (from 0 to 240 s in 15 s intervals) after sonication ended. The uptake of fluorescent molecules after sonication ended showed that increased cell permeability is long-lived and reversible over a timescale of seconds to minutes (Fig. 1c). During the recovery process, intracellular transport decreased over time after sonication and this decay was more rapid for larger molecules. These recovery kinetics are similar to previous measurements in related studies (Lee et al. 1996; Deng et al. 2004).

These data suggest that ultrasound may increase cell permeability by transiently altering plasma membrane integrity, which would be consistent with candidate mechanisms related to cell wounding and electroporation. We investigated this possibility by microscopic imaging of sonicated cells using electron and optical microscopy.

Cells exposed to ultrasound show changes in morphology similar to cell membrane wounds

To directly observe the effects of ultrasound exposure on cell membranes, DU 145 prostate cancer cells were images using multiple types of microscopy, including SEM, TEM, and laser-scanning confocal microscopy. Nonsonicated cells imaged by SEM have normal morphologic characteristics, including numerous microvilli (Figs. 2a1–2b1) (Gilloteaux et al. 1995). Sonicated cells, however, show localized effects to the

plasma membrane, including micron-sized changes in surface morphology (Fig. 2a2) that at higher magnification (Fig. 2a3) have structure similar to previous images of cytoskeleton (Svitkina et al. 1995). This suggests that patches of plasma membrane have been removed.

Other cells have dark areas lacking normal membrane morphology and containing dense populations of small vesicles, possibly indicating wound repair mechanisms described below (Figs. 2b2–2b3). To complement SEM images, TEM imaging of sonicated cells also shows breaks in plasma membrane continuity (Fig. 2c2), where vesicles are again associated with the disruption (Fig. 2c3). TEM of nonsonicated cells (Fig. 2c1) reveals continuous plasma membranes.

To further study plasma membrane changes, we used red-fluorescent wheat-germ lectin to label plasma membranes before sonication. Laser-scanning confocal microscopy of nonsonicated cells shows a ring of red fluorescence, indicating an intact plasma membrane, and no intracellular uptake when simultaneously exposed to green-fluorescent calcein used as a transport marker that normally cannot enter cells (Fig. 3a2). In contrast, cells imaged seconds after sonication can show large breaks in the plasma membrane ring similar to TEM imaging above. Uptake of calcein occurs in these cells (Fig. 3a4), possibly by transport through the plasma membrane disruption. A similar gap in membrane integrity is seen by brightfield microscopy (Fig. 3a3). These changes are seen in cells fixed within seconds after sonication and in viable cells imaged in real time. The fraction of cells showing these membrane effects by confocal microscopy (Fig. 3a) is similar to the fraction showing intracellular uptake by flow cytometry, *e.g.*, 10 to 40% (Fig. 1b).

Although confocal microscopy indicates that a

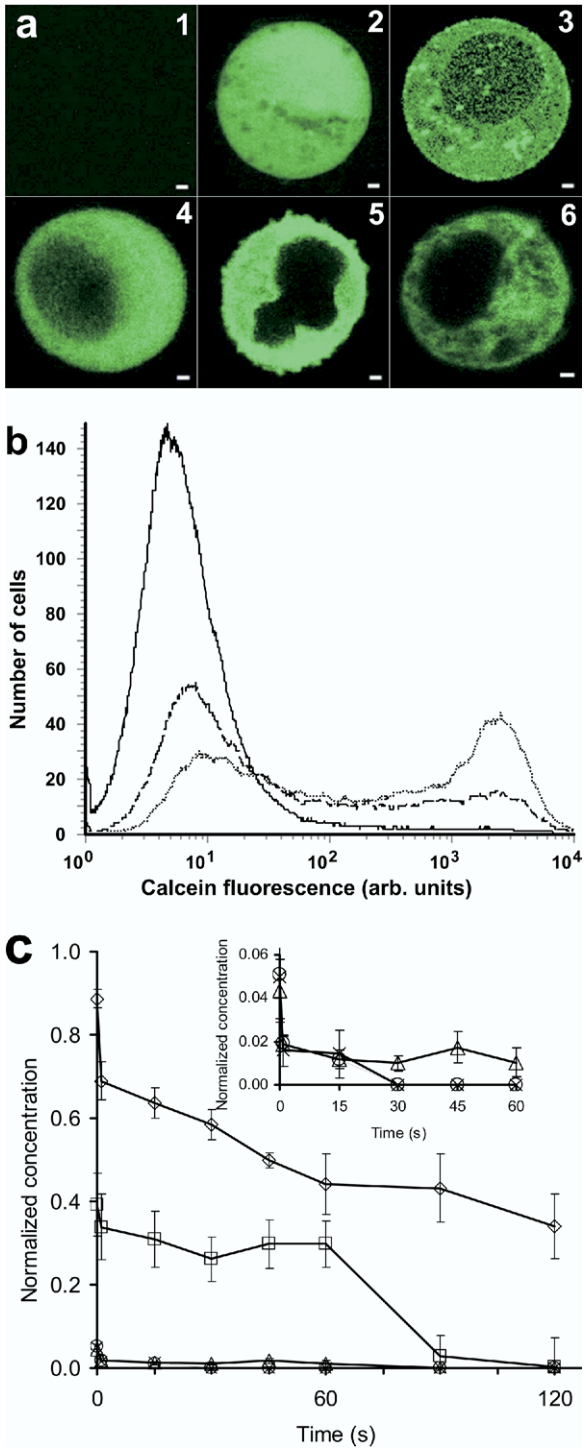

Fig. 1. Intracellular delivery by ultrasound. (a) Confocal micrographs showing a nonsonicated DU 145 cell exposed to calcein (A1) and sonicated cells exhibiting uptake of calcein (A2), bovine serum albumin (A3) and 150 (A4), 500 (A5) and 2,000 kDa (A6) dextrans. Scale bars are 1 μm; (b) flow cytometry uptake histograms of cells sonicated in buffer and incubated in calcein 1 s (dashed line), 30 s (dotted line) or 120 s (solid line) after sonication. Histograms show a population of cells with background fluorescence and a second population of cells with elevated fluorescence due to intracellular uptake of calcein; and (c) intracellular concentration as a function of time after sonication for calcein (623 Da, diamond), bovine serum albumin (66 kDa, square), and dextrans (150 kDa, triangle; 500 kDa, circle; 2,000 kDa, star). Cells were either sonicated with an uptake marker compound (time = 0 s) or in buffer alone, after which a marker compound was added at different times after sonication. Intracellular solute concentration determined by calibrated flow cytometry (Prausnitz et al. 1993) is normalized relative to its extracellular concentration (0.1 to 10 μM) and reported as the average value among viable cells affected by ultrasound. When normalized in this way, intracellular solute concentration is independent of extracellular concentration over the range considered (see Table 1f). Inset shows expanded view of dextran uptake at short times. Error bars show standard error of the mean.

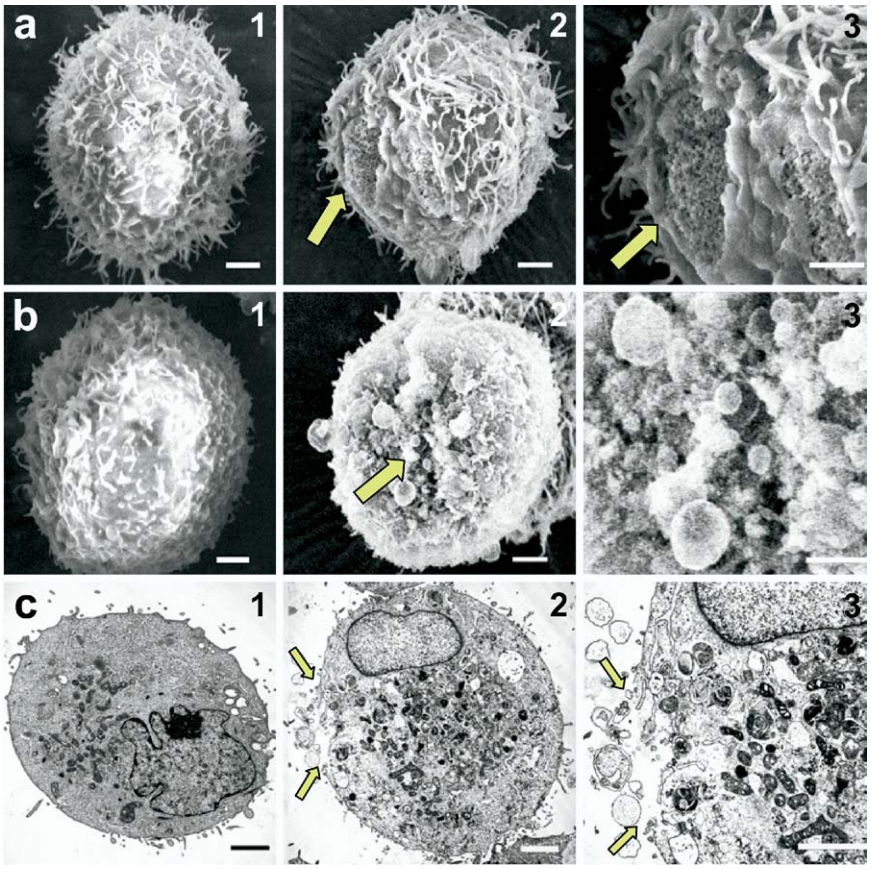

Fig. 2. Ultrastructural analysis of ultrasound's effect on plasma membrane. (a) Evidence of structural changes in plasma membrane due to ultrasound: SEM of (a1) nonsonicated DU 145 cell and (a2,a3) sonicated cell, shown at two levels of magnification, with a region lacking characteristic membrane surface topography and revealing exposed cytoskeleton; and (b, c) evidence of repairing wounds: SEM of (b1) nonsonicated cell and (b2,b3) sonicated cell, and TEM of (c1) nonsonicated cell and (c2,c3) sonicated cell, each with membrane disruption associated with numerous vesicles believed to be of intracellular origin and that may facilitate active membrane resealing. Cells were fixed 2 s after sonication using EM-grade glutaraldehyde (Castejon et al. 2001). Scale bars are 1 μm.

patch of labeled membrane was removed, we believe it was subsequently repaired because (1) calcein was retained inside the cell without leaking out during washing (Fig. 3a6); (2) assay with vital-stain propidium iodide showed that such cells remained viable with an intact membrane (data not shown); and (3) examination by brightfield and confocal microscopy revealed a continuous membrane in cells imaged minutes after sonication (Fig. 3a5–3a6). These morphologic observations are consistent with known cell-wound repair mechanisms, where pieces of removed plasma membrane are replaced by rapidly exocytosed vesicles that fuse with each other and actin cytoskeleton to form repair "patches" (Terasaki et al. 1997). These observations of removal and repair of micron-scale membrane patches are not consistent with electroporation, which involves formation of many distributed membrane pores of nanometer dimensions (Weaver and Chizmadzhev 1996), or with membrane invaginations associated with endocytosis (Alberts et al. 2002). Previous microscopic images have also shown changes to plasma membranes after sonication (Alter et al. 1998; Saito et al. 1999; Ogawa et al. 2001).

Sonicated cells lose internal vesicles, suggesting repair of wounds

This analysis suggests that ultrasound-mediated wounds in cells are capable of repair. During repair of cellular wounds generated by other physical forces, such as high-velocity fluid flow or mechanical scraping, pools of vesicles converge upon the wounded site and fuse to create repair patches (Terasaki et al. 1997). To determine if this process occurs in sonicated cells, we supplemented the electron microscopy images showing vesicles associated with wound sites (Fig. 2) with imaging by confo-

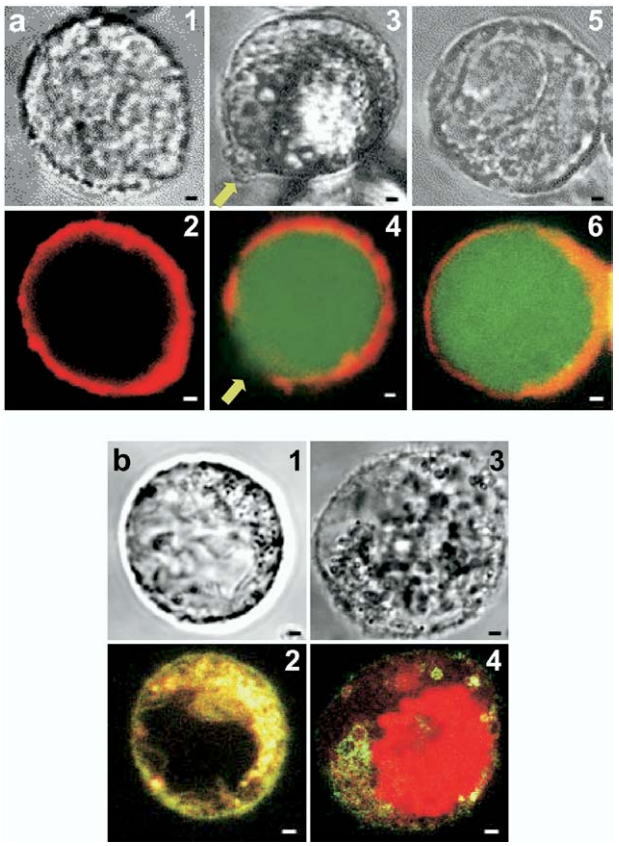

Fig. 3. Confocal fluorescence and brightfield microscopy of intracellular uptake and wound repair. (a) Labeling plasma membrane with red-fluorescent (TRITC) wheat-germ lectin (Sharon and Lis 1989) and sonicating in presence of calcein, a green-fluorescent transport marker, yields (a1, a2) nonsonicated DU 145 cell with intact membrane labeling and absence of intracellular calcein, which is expected in a normal, viable cell; (a3, a4) sonicated cell with a region of cell membrane removed and uptake of calcein imaged in cells fixed 2 s after sonication; and (a5, a6) sonicated cell with intact membrane labeling and uptake of calcein imaged in cells fixed 5 min after sonication; and (b) labeling intracellular vesicles with green fluorescent FM 1-43 (Cochilla et al. 1999) and sonicating in the presence of propidium iodide, a red-fluorescent transport marker that stains nuclei, yields (b1, b2) nonsonicated cell containing intracellular vesicles with intact plasma membrane; and (b3, b4) sonicated cell with partially depleted intracellular vesicles and plasma membrane that was breached, as shown by intracellular labeling with propidium iodide. Scale bars are 1 μm.

cal microscopy (Fig. 3b). After labeling the intracellular vesicle pool with the green-fluorescent dye FM 1-43, vesicle trafficking was monitored immediately after sonication.

Cells were initially filled with brightly labeled vesicles that substantially disappeared within a few minutes after sonication (Fig. 3b4). These kinetics are similar to the timescale of postsonication uptake of molecules (Fig. 1b). Because fluorescence of the FM 1-43 label dramatically decreases upon vesicle fusion with plasma membrane (Cochilla et al. 1999), this loss of fluorescence indicates vesicle trafficking and resealing of a membrane wound. These same cells took up a red-fluorescent transport marker that normally cannot enter cells (Fig. 3b4) and showed membrane breaks by wheat-germ lectin labeling (data not shown), which confirms that membrane disruption had occurred. Nonsonicated cells showed insignificant loss of vesicle fluorescence over time and no uptake of transport marker (Fig. 3b2).

Uptake and retention of molecules after sonication requires energy and calcium, which is consistent with recovery from cell membrane wounds

Previous studies have shown that cellular wound healing is an active process requiring ATP energy and elevated intracellular Ca^{2+} (McNeil and Terasaki 2001). To determine the role of energy-intensive processes after sonication, cells were depleted of ATP and exposed to ultrasound in presence of calcein. Energy-depleted cells were unable to retain calcein and had significantly lower viability than nondepleted cells sonicated at similar conditions, suggesting an inability to reseal ultrasound-mediated wounds (Table 1a).

To determine the role of Ca^{2+}, cells were treated with a Ca^{2+} chelator and exposed to ultrasound in presence of calcein. Ca^{2+}-depleted cells exhibited insignificant levels of uptake and had lower viability than nontreated cells sonicated at similar conditions, suggesting that postsonication membrane repair depends upon Ca^{2+} (Table 1b).

Ultrasound-mediated uptake does not occur in erythrocyte ghosts, suggesting a mechanism different from electroporation

To further study the role of cellular processes in ultrasound-mediated uptake, bovine erythrocyte ghosts were exposed to ultrasound over a range of conditions. In contrast to DU 145 cells, erythrocyte ghosts showed no uptake of calcein at any condition tested (Table 1c). Large cell wounds would not be expected to repair in erythrocyte ghosts, in part because they lack wound-repair machinery and endomembrane cytoskeletal components known to be required for active resealing (McNeil et al. 2003).

However, ghosts from similar samples could be loaded with calcein using electroporation (data not shown). Electroporation-mediated uptake of calcein and resealing of membranes is known to occur in erythrocyte ghosts (Chang et al. 1992), indicating that ultrasound-mediated uptake and retention occurs by a different mechanism. This conclusion is consistent

Table 1. Tests of mechanism of intracellular uptake by ultrasound

Test case*	Control	$C_{test}/C_{control}$ (%)†	Statistical significance‡
(a) Sonication with ATP depletion	Sonication with no treatment	2.2 ± 5	$p<0.01$
(b) Sonication with Ca^{2+} depletion	Sonication with no treatment	3.1 ± 2	$p<0.01$
(c) Sonication of erythrocyte ghosts	Sham sonication of erythrocyte ghosts	98.2 ± 5	$p>0.10$
(d) Sonication with K^+ depletion	Sonication with no treatment	96.5 ± 3	$p>0.10$
(e) Sonication with endocytic vesicle tracking (FM1-43)	Sham sonication with endocytic vesicle tracking (FM1-43)	101 ± 4	$p>0.10$
(f) Intracellular calcein concentration after sonication	Extracellular calcein concentration	104 ± 4	$p>0.10$
(g) Sonication after intracellular loading of calcein AM	Sham sonication after intracellular loading of calcein AM	40.0 ± 1.6	$p<0.01$
(h) Sonication with exocytic vesicle tracking (FM1-43)	Sham sonication with exocytic vesicle tracking (FM1-43)	81.5 ± 0.9	$p<0.01$

* DU 145 cells were treated as indicated before sonication in the presence of calcein, except for the case when erythrocyte ghosts were used instead.
† Intracellular calcein concentration of test-case cells (C_{test}) is normalized relative to control cells ($C_{control}$). 100% means no difference between C_{test} and $C_{control}$.
‡ A Student's *t*-test was performed to determine the significance of differences between C_{test} and $C_{control}$.

with previous microscopy images showing membrane defects caused by electroporation on the 1- to 100-nm lengthscale (Chang and Reese 1990), which contrast with the micron-scale effects seen here (Figs. 2 and 3).

Ultrasound-mediated uptake does not depend on potassium or vesicle internalization, suggesting a mechanism different from endocytosis

To further rule out a mechanism based on endocytosis, cells were depleted of K^+, an essential component of both clathrin-coated pits and caveoli, using K^+-free buffer after hypotonic shock. After ultrasound exposure, calcein uptake by K^+-depleted cells was indistinguishable from nontreated cells (Table 1d). Furthermore, plasma membranes intercalated with vesicle stain FM 1-43 before sonication showed no evidence of induced endocytosis, as determined by unchanged intracellular levels of fluorescence from internalized labeled vesicles after sonication (Table 1e).

Additional characterization of ultrasound-induced wounds

Additional experiments demonstrated that intracellular uptake scaled proportionally with extracellular calcein concentration between 1 to 1000 μM (Table 1f), which is consistent with concentration-dependent diffusion, or convection, through membrane disruptions. Moreover, cells loaded with calcein AM before sonication were significantly depleted of their intracellular calcein after sonication (Table 1g), demonstrating that ultrasound causes bidirectional transport across the plasma membrane. Finally, consistent with the qualitative image in Fig. 3b4, cells quantitatively lost a large fraction of intracellular vesicle stores after sonication (Table 1h), which is expected for vesicle-mediated repair of membrane wounds.

DISCUSSION

Ultrasound-mediated uptake is mechanistically related to cell membrane wounding

Altogether, these data suggest that the mechanism by which ultrasound delivers molecules into cells is related to cell membrane wounding generated by other physical forces (McNeil and Steinhardt 2003). Ultrasound's effects are characterized by a transient increase in concentration-dependent, bidirectional transport of macromolecules into the cytosol that are associated with micron-scale disruptions in plasma membranes. Uptake due to membrane resealing and cell recovery involves ATP, Ca^{2+}, intracellular vesicles and wound-repair machinery not present in erythrocyte ghosts, but does not require K^+ or endocytic activity. These findings are all consistent with known characteristics of cell membrane wounds.

In contrast, these findings are not consistent with intracellular uptake from electroporation or endocytosis. Electroporation is a physical phenomenon that occurs in nonliving bilayer systems, which permits access to the cytosol through 1- to 10-nm-size pores in the plasma membrane that spontaneously reseal without the involvement of ATP, Ca^{2+}, intracellular vesicles or special wound-repair machinery (Chang et al. 1992). Endocytosis is an energy-dependent process mediated by membrane invaginations that does not involve micron-scale transmembrane pores, Ca^{2+}-mediated processes or bidirectional transport and does require endocytic activity and often K^+ (Yeagle 1993).

Significance of mechanism for drug delivery and other applications

Cell membranes pose one of the greatest barriers to delivery of drugs, proteins, DNA and other molecules into cells and tissues. The ability of ultrasound to transiently disrupt these barriers in living cells could provide

an important tool, especially for delivery of macromolecular drugs or other compounds requiring access to the cytosol. The fact that ultrasound can be focused almost anywhere in the body using an extracorporeal device offers the additional possibility of noninvasive targeting of therapy to specific tissues or locations in the body.

The relatively large size of ultrasound-created disruptions indicates that this method could be used not only to deliver a broad range of compounds, such as drugs, proteins, DNA and RNA (Dalecki 2004; Tachibana 2004), but might also be applicable to small particles, such as polymeric particles, chromosomes and other macromolecular complexes. The nonspecific nature of the transport mechanism suggests a large breadth of application, where specificity can be achieved by spatial targeting of the ultrasonic energy, rather than having to identify and exploit differences between cell types, receptor-ligand pairings, or other hard-to-control parameters that are pursued in other targeting methods (Langer 1998).

Although not addressed in this study, cell death associated with ultrasound treatment constrains applications. The mechanism of membrane disruption and resealing suggests methods to reduce cell death by promoting membrane repair. Endogenous repair mechanisms could be upregulated or compounds could be added to provide a membrane patch using exogenous materials. Other studies suggest that cell membrane wounding is a phenomenon that occurs routinely in the human body as a part of normal physiology (McNeil and Steinhardt 2003), indicating that ultrasound-mediated wounding has the potential to be developed as a safe method of drug delivery.

Finally, although the noninvasive nature of ultrasound exposure is attractive for many applications, the cell membrane wounding mechanism described here suggests that ultrasound and acoustic cavitation are not the only ways to drive molecules into cells by this mechanism. Wounding can be achieved by a variety of different physical stresses to the cell membrane (McNeil and Steinhardt 2003), and other methods to physically disrupt cell membranes may be preferable for certain applications.

CONCLUSIONS

Overall, this study shows that ultrasound induces extensive intracellular uptake of molecules, including proteins and other macromolecules, and that, depending on molecular size, transport can persist for >1 min after sonication. Microscopy suggests a mechanism involving micron-scale wounds in the plasma membrane that reseal using intracellular vesicles by an energy-intensive process requiring Ca^{2+}. This mechanism appears similar to that previously reported for mechanical wounding of cells by other physical mechanisms and different from electroporation and endocytosis, which induce intracellular uptake by other processes. We therefore conclude that ultrasound-mediated uptake into cells occurs through plasma membrane wounds of up to micron dimensions that are repaired within minutes by vesicle exocytosis. Guided by knowledge of wound-repair mechanisms, ultrasound-based uptake into cells is a promising approach to noninvasively focus drug and gene delivery for biotechnology and clinical applications.

Acknowledgements—This manuscript is dedicated to the memory of our colleague and friend, Robert P. Apkarian. The authors thank M. Desai for laboratory assistance, J. D. Hutcheson for technical discussions and J.V. Taylor for electron microscopy sample preparation. This work was supported in part by the National Science Foundation and the National Institutes of Health. RKS, HR, TPT, VZ and MRP are members of the Georgia Tech Institute for Bioengineering and Bioscience; RKS, TPT and MRP are members of the Georgia Tech Interdisciplinary Bioengineering Program; and RKS and MRP are members of the Georgia Tech/NIH Training Program in Cellular and Tissue Engineering. RKS carried out and helped design and analyze all experiments. HR helped design experiments and interpret results concerning cellular responses to ultrasound. TPT helped carry out confocal imaging experiments and their interpretation. RPA helped design, implement and interpret electron microscopy studies. VZ helped analyze cellular uptake data. MRP helped design and interpret all aspects of the study and served as the principal investigator.

REFERENCES

Alberts B, Johnson A, Lewis J, Raff M, Roberts K, Walter P. Molecular Biology of the Cell. New York: Garland Science, 2002.

Alter A, Rozenszajn LA, Miller HI, Rosenschein U. Ultrasound inhibits the adhesion and migration of smooth muscle cells in vitro. Ultrasound Med Biol 1998;24:711–721.

Arndt-Jovin DJ, Jovin TM. Fluorescence labeling and microscopy of DNA. Methods Cell Biol 1989;30:417–448.

Bekeredjian R, Grayburn PA, Shohet RV. Use of ultrasound contrast agents for gene or drug delivery in cardiovascular medicine. J Am Coll Cardiol 2005;45:329–335.

Castejon OJ, Castejon HV, Apkarian RP. Confocal laser scanning, conventional scanning and transmission electron microscopy of vertebrate cerebellar granule cells. Biocell 2001;25:235–255.

Chang DC, Chassy BM, Saunders JA, Sowers AE, eds. Guide to Electroporation and Electrofusion. New York: Academic Press, 1992.

Chang DC, Reese TS. Changes in membrane structure induced by electroporation as revealed by rapid-freezing electron microscopy. Biophys J 1990;58:1–12.

Chen JL, Ahluwalia JP, Stamnes M. Selective effects of calcium chelators on anterograde and retrograde protein transport in the cell. J Biol Chem 2002;277:35682–35687.

Cochilla AJ, Angleson JK, Betz WJ. Monitoring secretory membrane with FM1–43 fluorescence. Annu Rev Neurosci 1999;22:1–10.

Cochran SA, Prausnitz MR. Sonoluminescence as an indicator of cell membrane disruption by acoustic cavitation. Ultrasound Med Biol 2001;27:841–850.

Dalecki D. Mechanical bioeffects of ultrasound. Annu Rev Biomed Eng 2004;6:229–248.

Deng CX, Sieling F, Pan H, Cui J. Ultrasound-induced cell membrane porosity. Ultrasound Med Biol 2004;30:519–526.

Dodge JT, Mitchell C, Hanahan DJ. The preparation and chemical characteristics of hemoglobin-free ghosts of human erythrocytes. Arch Biochem Biophys 1963;100:119–130.

Fechheimer M, Boylan JF, Parker S, Sisken JE, Patel FL, Zimmer SG. Transfection of mammalian cells with plasmid DNA by scrape loading and sonication loading. Proc Natl Acad Sci U S A 1987; 84:8463–8467.

Gao DY, Benson CT, Liu C, McGrath JJ, Critser ES, Critser JK. Development of a novel microfusion chamber for determination of cell membrane transport properties. Biophys J 1996;71:443–450.

Gilloteaux J, Jamison JM, Venugopal M, Giammar D, Summers JL. Scanning electron microscopy and transmission electron microscopy aspects of synergistic antitumor activity of vitamin C – vitamin K3 combinations against human prostatic carcinoma cells. Scanning Microsc 1995;9:159–173.

Gonzalez-Dunia D, Cubitt B, de la Torre JC. Mechanism of Borna disease virus entry into cells. J Virol 1998;72:783–788.

Guzman HR, McNamara AJ, Nguyen DX, Prausnitz MR. Bioeffects caused by changes in acoustic cavitation bubble density and cell concentration: A unified explanation based on cell-to-bubble ratio and blast radius. Ultrasound Med Biol 2003;29:1211–1222.

Guzman HR, Nguyen DX, Khan S, Prausnitz MR. Ultrasound-mediated disruption of cell membranes II: Heterogeneous effects on cells. J Acoust Soc Am 2001;110:597–606.

Hill CR, Bamber JC, ter Haar GR, eds. Physical Principles of Medical Ultrasonics. New York: Wiley, 2004.

Huber PE, Mann MJ, Melo LG, et al. Focused ultrasound (HIFU) induces localized enhancement of reporter gene expression in rabbit carotid artery. Gene Ther 2003;10:1600–1607.

Keminer O, Peters R. Permeability of single nuclear pores. Biophys J 1999;77:217–228.

Langer R. Drug delivery and targeting. Nature 1998;392:5–10.

Larina IV, Evers BM, Esenaliev RO. Optimal drug and gene delivery in cancer cells by ultrasound-induced cavitation. Anticancer Res 2005;25:149–156.

Larkin JM, Brown MS, Goldstein JL, Anderson RG. Depletion of intracellular potassium arrests coated pit formation and receptor-mediated endocytosis in fibroblasts. Cell 1983;33:273–285.

Lee S, Anderson T, Zhang H, Flotte TJ, Doukas AG. Alteration of cell membrane by stress waves in vivo. Ultrasound Med Biol 1996;22: 1285–1293.

McCreery TP, Sweitzer RH, Unger EC, Sullivan S. DNA delivery to cells in vivo by ultrasound. Methods Mol Biol 2004;245:293–298.

McNeil PL, Miyake K, Vogel SS. The endomembrane requirement for cell surface repair. Proc Natl Acad Sci U S A 2003;100:4592–4597.

McNeil PL, Steinhardt RA. Plasma membrane disruption: repair, prevention, adaptation. Annu Rev Cell Dev Biol 2003;19:697–731.

McNeil PL, Terasaki M. Coping with the inevitable: How cells repair a torn surface membrane. Nat Cell Biol 2001;3:E124–E129.

Mitragotri S, Kost J. Low-frequency sonophoresis: A review. Adv Drug Deliv Rev 2004;56:589–601.

Ogawa K, Tachibana K, Uchida T, et al. High-resolution scanning electron microscopic evaluation of cell-membrane porosity by ultrasound. Med Electron Microsc 2001;34:249–253.

Ohl CD, Wolfrum B. Detachment and sonoporation of adherent HeLa-cells by shock wave-induced cavitation. Biochim Biophys Acta 2003;1624:131–138.

Prausnitz MR, Lau BS, Milano CD, Conner S, Langer R, Weaver JC. A quantitative study of electroporation showing a plateau in net molecular transport. Biophys J 1993;65:414–422.

Prentice P, Cuschieri A, Dholakia K, Prausnitz M, Campbell P. Membrane disruption by optically controlled microbubble cavitation. Nature Physics 2005;1:107–110.

Rapley R, Walker J, eds. Molecular Biomethods Handbookq. Totowa, NJ: Humana Press, 1998.

Saito K, Miyake K, McNeil PL, Kato K, Yago K, Sugai N. Plasma membrane disruption underlies injury of the corneal endothelium by ultrasound. Exp Eye Res 1999;68:431–437.

Sharon N, Lis H. Lectins as cell recognition molecules. Science 1989; 246:227–234.

Svitkina TM, Verkhovsky AB, Borisy GG. Improved procedures for electron microscopic visualization of the cytoskeleton of cultured cells. J Struct Biol 1995;115:290–303.

Tachibana K. Emerging technologies in therapeutic ultrasound: Thermal ablation to gene delivery. Hum Cell 2004;17:7–15.

Terasaki M, Miyake K, McNeil PL. Large plasma membrane disruptions are rapidly resealed by Ca^{2+}-dependent vesicle-vesicle fusion events. J Cell Biol 1997;139:63–74.

Togo T, Alderton JM, Bi GQ, Steinhardt RA. The mechanism of facilitated cell membrane resealing. J Cell Sci 1999;112:719–731.

Tomizawa M, Ebara M, Saisho H, Sakiyama S, Tagawa M. Irradiation with ultrasound of low output intensity increased chemosensitivity of subcutaneous solid tumors to an anti-cancer agent. Cancer Lett 2001;173:31–35.

van Wamel A, Bouakaz A, Versluis M, de Jong N. Micromanipulation of endothelial cells: Ultrasound-microbubble-cell interaction. Ultrasound Med Biol 2004;30:1255–1258.

Weaver JC, Chizmadzhev YA. Theory of electroporation: A review. Bioelectrochem Bioenerget 1996;41:135–160.

Yeagle PL. The Membranes of Cells. San Diego: Academic Press, 1993.

Yuh EL, Shulman SG, Mehta SA, et al. Delivery of systemic chemotherapeutic agent to tumors by using focused ultrasound: study in a murine model. Radiology 2005;234:431–437.

Zarnitsyn VG, Prausnitz MR. Physical parameters influencing optimization of ultrasound-mediated DNA transfection. Ultrasound Med Biol 2004;30:527–538.